

Can the Two-Higgs-Doublet Model Survive the Constraint from the Muon Anomalous Magnetic Moment as Suggested ?

Kingman Cheung¹ and Otto C. W. Kong²

¹*National Center for Theoretical Sciences,*

National Tsing Hua University, Hsinchu, Taiwan.

²*Department of Physics, National Central University, Chung-li, Taiwan 32054*

Email: cheung@phys.cts.nthu.edu.tw & otto@phy.ncu.edu.tw

Abstract

Requiring the two-Higgs-doublet model II to accommodate the 3σ deviation in the muon anomalous magnetic moment imposes specific constraints on the Higgs spectrum. We analyze the combination of all the relevant, available, constraints on the model parameter space. The use of constraints from $b \rightarrow s\gamma$, the precision electroweak measurements of R_b , and the ρ parameter, together with exclusions from direct searches at LEP, give extremely severe restrictions on the model parameters. That is “almost enough” to kill the model altogether. The exclusion would be even stronger if the direct searches can be optimized to complement the other constraints, as will be discussed in details in this work.

PACS numbers:

I. INTRODUCTION

Physicists have been delighted by the extraordinary success of the standard model (SM), while many got frustrated by the lack of experimental clues for the construction of the theory beyond. The most recent measurement on the muon anomalous magnetic moment a_μ revealed a deviation as large as 3σ from the SM prediction. This has no doubt been taken as a strong suggestion for physics beyond the SM. Since many extensions of the SM are capable of giving rise to such a deviation, theorists, typically, would like to check the constraints imposed on the parameter space of a specific model. Such constraints are particularly interesting, because they are likely to give information not only on excluded regions but also on the predictions for where else should other evidences on the model be expected. For example, one expects to find a lower bound on the mass of a new particle playing the role on generating the extra contribution to a_μ . The information has especially strong implications on models that have a small number of parameters which are already stringently constrained by various precision electroweak data.

One of the simplest extensions of the SM is the two-Higgs-doublet model (2HDM) [1], which adds one Higgs doublet in addition to the one required in the SM. A generic 2HDM allows flavor-changing neutral currents (FCNC), which can be avoided by restricting the couplings of the doublets, say, by imposing an *ad hoc* discrete symmetry[2]. The most popular version, known as model II, has one Higgs doublet coupled to the down-type quarks (and charged leptons) and the second doublet to the up-type quarks. The physical content of the Higgs sector (assuming no CP violation) includes a pair of CP-even neutral Higgs bosons H and h , a CP-odd neutral boson A , and a pair of charged-Higgs bosons H^\pm . The model fits in well with the criteria mentioned above for the a_μ result to have a very strong impact. We focus on the 2HDM II in this paper, answering the question of to what extent the model can survive a requirement of generating the 3σ deviation in a_μ , as suggested.

The 2HDM II has been extensively studied in literature and tested experimentally. One of the most stringent tests is the radiative decay of B mesons, specifically, the inclusive decay rate of $b \rightarrow s \gamma$, which has the least hadronic uncertainties. In the 2HDM, the rate of $b \rightarrow s \gamma$ can be enhanced substantially for large regions in the parameter space of the mass m_{H^\pm} of the charged-Higgs boson and $\tan\beta(= v_2/v_1$, where v_1 and v_2 are the vacuum expectation values of the down- and up-sector Higgs doublets, respectively). An earlier analysis has already put a constraint on the charged-Higgs boson mass at $m_{H^\pm} > 380$ GeV[3] (see also Ref.[4]). Updating the constraint while asking for the model to give rise to the a_μ deviation as suggested already imposes a strong and specific mass hierarchy between the pseudoscalar and the charged scalar. Electroweak precision data also have strong implications on the model.

The 2HDM can explain the muon anomalous magnetic moment deviation with a light pseudoscalar boson A contributing via a 2-loop Barr-Zee-type diagram [5, 6]. Our interest here is in updating a previous analysis[6] and extending it to a comprehensive treatment of

all the relevant constraints. The OPAL Collaboration has recently published an update on their search for the Higgs bosons within the 2HDM framework. Since their result is more stringent than before, by combining the updated constraints from a_μ and other precision measurements, such as the ρ parameter, R_b , and the $b \rightarrow s\gamma$ rate, together with this new OPAL result and a study on Yukawa processes from DELPHI, we are able to limit the 2HDM to a tiny window of parameter space with an, perhaps, uncomfortably large value of $\tan\beta$. All in all, we will piece together a story of the very stringently constrained 2HDM, almost to the extent of killing it altogether.

Our presentation of the constraints follows what we consider the most efficient way to appreciate the overall results. The organization is as follows. In the next section we briefly describe the 2HDM (II) and the relevant parameters used in our analysis. In Sec. III, we look at the $b \rightarrow s\gamma$ rate and the $B^0 - \overline{B}^0$ mixing, which require a heavy charged Higgs boson. In Sec. IV, we discuss the Higgs-sector contributions to a_μ and R_b , and show the strongly complementary character of the two data and how that plays off in the 2HDM. We give our fits to the data, with the exclusions from DELPHI and OPAL further imposed. In Sec. V, we add the consideration of the ρ parameter. We conclude in Sec. VI.

II. PARAMETER SPACE OF THE TWO HIGGS DOUBLET MODEL II

We take the parameter space of the model as given by a set of six Higgs-sector parameters

$$m_h, m_H, m_A, m_{H^\pm}, \tan\beta, \text{ and } \alpha.$$

Here, the first four are masses of the physical Higgs states. The last one, α , is the real scalar Higgs mixing angle as defined in Ref.[1]. We would like to emphasize that we are taking this set of six parameters as mutually independent experimental parameters. From the theoretical point of view, one has parameters in the scalar potential from which the above can be derived. However, without supersymmetry or anything else to avoid the hierarchy problem, the masses for the Higgs states suffer from quadratic divergences. The tree-level relations among parameters are modified substantially by loop corrections which depend on the renormalization approach and the cut-off imposed. To stay away from such uncertainties, we do not discuss the scalar potential here, except noting that there are enough degrees of freedom in the model in general, and especially with the loop corrections taken into account, to allow us to take the above six parameters as mutually independent.

The four physical masses are direct experimentally measurable quantities. The other two parameters, $\tan\beta$ and the angle α , come into the game as effective couplings. The Yukawa couplings of h, H , and A to up- and down-type quarks are given by, with a common factor

of $-igm_f/2M_W$,

	$t\bar{t}$	$b\bar{b}$	$\tau^-\tau^+$
h :	$\cos\alpha/\sin\beta$	$-\sin\alpha/\cos\beta$	$-\sin\alpha/\cos\beta$
H :	$\sin\alpha/\sin\beta$	$\cos\alpha/\cos\beta$	$\cos\alpha/\cos\beta$
A :	$-i\cot\beta\gamma_5$	$-i\tan\beta\gamma_5$	$-i\tan\beta\gamma_5$

while the charged Higgs H^- couples to t and \bar{b} via

$$\bar{b}tH^- : \frac{ig}{2\sqrt{2}M_W} [m_t \cot\beta (1 + \gamma_5) + m_b \tan\beta (1 - \gamma_5)] .$$

From the perspective of our study here, the couplings given above may be considered as defining implicitly the two parameters $\tan\beta$ and α . Other relevant couplings in our study are those to gauge bosons, as given by,

$$\begin{aligned} hZZ &: ig M_Z \frac{\sin(\beta - \alpha)}{\cos\theta_W} g^{\mu\nu} \\ HZZ &: ig M_Z \frac{\cos(\beta - \alpha)}{\cos\theta_W} g^{\mu\nu} \\ hAZ &: g \frac{\cos(\beta - \alpha)}{2 \cos\theta_W} (p - p')^\mu \\ HAZ &: -g \frac{\sin(\beta - \alpha)}{2 \cos\theta_W} (p - p')^\mu \\ H^+H^-Z &: -ig \frac{\cos 2\theta_W}{2 \cos\theta_W} (p - p')^\mu , \end{aligned}$$

where $p(h, H, H^+)$ and $p'(A, H^-)$ are the 4-momenta going into the vertex.

III. REQUIREMENT OF A HEAVY CHARGED HIGGS BOSON

It has been well appreciated that B physics bars the 2HDM from admitting a relatively light charged-Higgs state. We first review the constraints here. The first important constraint comes from the inclusive $B \rightarrow X_s \gamma$ result, and the second one comes from the $B^0 - \bar{B}^0$ mixing. The essential point here is that without a direct source of FCNC, the charged Higgs mediates the only significant contributions to flavor-changing processes, in addition to the W^\pm -mediated SM process. The experimental data then allows us to bound the charged Higgs mass independent of the other Higgs states.

The detail description of the effective Hamiltonian approach can be found in Refs. [7, 8]. Here we present the highlights that are relevant to our discussions. The effective Hamiltonian for $B \rightarrow X_s \gamma$ at a factorization scale of order $O(m_b)$ is given by

$$\mathcal{H}_{\text{eff}} = -\frac{G_F}{\sqrt{2}} V_{ts}^* V_{tb} \left[\sum_{i=1}^6 C_i(\mu) Q_i(\mu) + C_{7\gamma}(\mu) Q_{7\gamma}(\mu) + C_{8G}(\mu) Q_{8G}(\mu) \right] . \quad (1)$$

The operators Q_i can be found in Ref.[7], of which the Q_1 and Q_2 are the current-current operators and $Q_3 - Q_6$ are QCD penguin operators. $Q_{7\gamma}$ and Q_{8G} are, respectively, the magnetic penguin operators specific for $b \rightarrow s \gamma$ and $b \rightarrow s g$. Here we also neglect the mass of the external strange quark compared to the external bottom-quark mass.

The decay rate of $B \rightarrow X_s \gamma$ normalized to the experimental semileptonic decay rate is given by

$$\frac{\Gamma(B \rightarrow X_s \gamma)}{\Gamma(B \rightarrow X_c e \bar{\nu}_e)} = \frac{|V_{ts}^* V_{tb}|^2}{|V_{cb}|^2} \frac{6 \alpha_{\text{em}}}{\pi f(m_c/m_b)} |C_{7\gamma}(m_b)|^2, \quad (2)$$

where $f(z) = 1 - 8z^2 + 8z^6 - z^8 - 24z^4 \ln z$. The Wilson coefficient $C_{7\gamma}(m_b)$ is given by

$$C_{7\gamma}(\mu) = \eta^{\frac{16}{23}} C_{7\gamma}(M_W) + \frac{8}{3} \left(\eta^{\frac{14}{23}} - \eta^{\frac{16}{23}} \right) C_{8G}(M_W) + C_2(M_W) \sum_{i=1}^8 h_i \eta^{a_i}, \quad (3)$$

where $\eta = \alpha_s(M_W)/\alpha_s(\mu)$. The a_i 's and h_i 's can be found in Ref. [7]. The coefficients $C_i(M_W)$ at the leading order in 2HDM II are given by

$$C_j(M_W) = 0 \quad (j = 1, 3, 4, 5, 6), \quad (4)$$

$$C_2(M_W) = 1, \quad (5)$$

$$C_{7\gamma}(M_W) = -\frac{A(x_t)}{2} - \frac{A(y_t)}{6} \cot^2 \beta - B(y_t), \quad (6)$$

$$C_{8G}(M_W) = -\frac{D(x_t)}{2} - \frac{D(y_t)}{6} \cot^2 \beta - E(y_t), \quad (7)$$

where $x_t = m_t^2/M_W^2$, and $y_t = m_t^2/m_{H^\pm}^2$. The Inami-Lim functions[9] are given by

$$A(x) = x \left[\frac{8x^2 + 5x - 7}{12(x-1)^3} - \frac{(3x^2 - 2x) \ln x}{2(x-1)^4} \right], \quad (8)$$

$$B(y) = y \left[\frac{5y - 3}{12(y-1)^2} - \frac{(3y-2) \ln y}{6(y-1)^3} \right], \quad (9)$$

$$D(x) = x \left[\frac{x^2 - 5x - 2}{4(x-1)^3} + \frac{3x \ln x}{2(x-1)^4} \right], \quad (10)$$

$$E(y) = y \left[\frac{y-3}{4(y-1)^2} + \frac{\ln y}{2(y-1)^3} \right]. \quad (11)$$

The most recent experimental data on $b \rightarrow s \gamma$ rate has been reported [10], giving

$$B(b \rightarrow s \gamma)|_{\text{exp}} = 3.88 \pm 0.36(\text{stat}) \pm 0.37(\text{sys})_{-0.28}^{+0.43}(\text{theory}).$$

The most updated SM prediction is [11]

$$B(b \rightarrow s \gamma)|_{\text{SM}} = (3.64 \pm 0.31) \times 10^{-4},$$

which agrees very well the data. Therefore, there is only a little room for new physics contributions. The constraint on new physics contribution is, explicitly,

$$\Delta B(b \rightarrow s \gamma) \equiv B(b \rightarrow s \gamma)|_{\text{exp}} - B(b \rightarrow s \gamma)|_{\text{SM}} = (0.24_{-0.59}^{+0.67}) \times 10^{-4}. \quad (12)$$

The quantity that parameterizes the $B^0 - \overline{B}^0$ mixing is

$$x_d \equiv \frac{\Delta m_B}{\Gamma_B} = \frac{G_F^2}{6\pi^2} |V_{td}^*|^2 |V_{tb}|^2 f_B^2 B_B m_B \eta_B \tau_B M_W^2 (I_{WW} + I_{WH} + I_{HH}) , \quad (13)$$

where[12]

$$\begin{aligned} I_{WW} &= \frac{x}{4} \left[1 + \frac{3-9x}{(x-1)^2} + \frac{6x^2 \log x}{(x-1)^3} \right] , \\ I_{WH} &= xy \cot^2 \beta \left[\frac{(4z-1) \log y}{2(1-y)^2(1-z)} - \frac{3 \log x}{2(1-x)^2(1-z)} + \frac{x-4}{2(1-x)(1-y)} \right] , \\ I_{HH} &= \frac{xy \cot^4 \beta}{4} \left[\frac{1+y}{(1-y)^2} + \frac{2y \log y}{(1-y)^3} \right] , \end{aligned}$$

with $x = m_t^2/M_W^2$, $y = m_t^2/m_{H^\pm}^2$, $z = M_W^2/m_{H^\pm}^2$, and the running top mass $m_t = m_t(m_t) = 166 \pm 5$ GeV. The experimental value is [13]

$$x_d = 0.755 \pm 0.015 . \quad (14)$$

We use the following input parameters [13]: $|V_{tb}V_{td}^*| = 0.0079 \pm 0.0015$, $f_B^2 B_B = (198 \pm 30 \text{ GeV})^2 (1.30 \pm 0.12)$, $m_B = 5279.3 \pm 0.7$ MeV, $\eta_B = 0.55$, and $\tau_B = 1.542 \pm 0.016$ ps. Note that the value of $|V_{tb}V_{td}^*|$ is in fact determined by the measurement of x_d . Now we can use the data to constrain the new contribution from the charged-Higgs boson.

The two constraints discussed above are quite stringent, giving a lower bound on m_{H^\pm} close to 500 GeV at 95% C.L. for intermediate and large values of $\tan\beta$. The result is illustrated in Fig. 1. The heavy charged Higgs mass means that the state pretty much decouples, playing a little role in the contributions of the 2HDM to quantities like a_μ and R_b , which we turn to in the next section.

IV. a_μ VS R_b

The most recent data on the a_μ indicates [14]¹

$$\Delta a_\mu \equiv a_\mu^{\text{exp}} - a_\mu^{\text{SM}} = (33.9 \pm 11.2) \times 10^{-10} . \quad (15)$$

The result shows a 3σ deviation to be explained by new physics. Adopting the view that the a_μ problem is real and demands new physics contributions, we will see that it has a strong and definite implication on the Higgs spectrum of the 2HDM. In fact, we had performed an analysis [6] along the line for the earlier data. The major point is that a light pseudoscalar, together with a large $\tan\beta$ value, is required to explain the positive Δa_μ

¹ This 3σ deviation was using the e^+e^- data. If the τ decay data are used, the deviation would be reduced to about 0.9σ [14], which, however, has model dependence and thus less reliable.

contribution via a two-loop Barr-Zee diagram [15]. A real scalar contributes in the negative direction. To avoid a cancellation, the real scalar mass has to be heavy. We will show here that such a mass splitting is strongly disfavored by the allowed contribution to R_b , for which the experimental data agrees well with the SM prediction. The two constraints are hence strongly complementary.

It has been emphasized in Ref.[5, 6] that for the Higgs boson mass larger than about 3 GeV, the dominant Higgs contributions to a_μ actually come from the two-loop Barr-Zee diagram with a heavy fermion (f) running in the upper loop. A m_f^2/m_μ^2 factor could easily overcome the $\alpha/4\pi$ loop factor. In our calculation here, we include all one-loop contributions and all two-loop Barr-Zee-type contributions with an internal photon and a third-family fermion running in the loop. The later diagrams are strongly enhanced by $\tan\beta$. If the internal photon was replaced by a W^\pm or a Z^0 , the contributions will be much suppressed (see [16], for examples). The W^\pm case is in particular strongly suppressed, partly as a result of the fact that the Higgs boson has to be H^\pm , the mass of which we have shown above to be heavier than 500 GeV. The only other important diagrams of the Barr-Zee type are the SM diagrams, such as the one with the W^\pm replacing the heavy fermion. We neglect the small “extra” contributions from such diagrams[17] because of the difference between the Higgs boson mass used here and that used in the a_μ^{SM} number[18].

Explicitly, we first write the fermion couplings of a neutral Higgs mass eigenstate ϕ^0 as

$$\mathcal{L}^{\bar{f}\phi^0 f} = -\lambda_f \frac{m_f}{v} \bar{f}\phi^0 f + i\gamma_5 A_f \frac{m_f}{v} \bar{f}\phi^0 f, \quad (16)$$

where $\lambda_f \frac{m_f}{v}$ and $A_f \frac{m_f}{v}$ are the effective scalar and pseudoscalar couplings, and $v = 246$ GeV. The two-loop photon Barr-Zee diagram contribution from ϕ^0 , with a heavy fermion f running in the second loop, is given by

$$\Delta a_\mu^\phi = \frac{N_c^f \alpha_{\text{em}} m_\mu^2}{4\pi^3 v^2} \mathcal{Q}_f^2 \left[A_\mu A_f g\left(\frac{m_f^2}{m_\phi^2}\right) - \lambda_\mu \lambda_f f\left(\frac{m_f^2}{m_\phi^2}\right) \right], \quad (17)$$

where

$$\begin{aligned} f(z) &= \frac{1}{2}z \int_0^1 dx \frac{1 - 2x(1-x)}{x(1-x) - z} \ln \frac{x(1-x)}{z}, \\ g(z) &= \frac{1}{2}z \int_0^1 dx \frac{1}{x(1-x) - z} \ln \frac{x(1-x)}{z}; \end{aligned} \quad (18)$$

N_c^f represents the number of color degrees of freedom in f , and \mathcal{Q}_f its electric charge. Here, we have three scalars and no CP violating mixing is assumed. The real scalars h and H give negative contributions only (from the second part) while a pseudoscalar A gives a positive contribution only (from the first part). The diagram is $\tan\beta$ enhanced, with an additional $\tan\beta$ factor for the b and τ loop compared to the t loop.

We plot in Fig. 2 the 2σ range of solution to a_μ on the plane of the pseudoscalar mass m_A versus $\tan\beta$, considering only the pseudoscalar contribution. Note that while the region below the solution band is excluded, the solution in the region above the band may

be admissible when the a_μ is compensated by some negative contributions from the real scalar(s). We also superimpose on the plot the excluded region from the DELPHI study on Higgs Yukawa processes in the $4b$ and $2b2\tau$ final states [19]. We can see that one obtains lower bounds on m_A and $\tan\beta$ as 26 GeV and 30 respectively, apart from the small window around $m_A = 10$ GeV and $\tan\beta = 20$.² We had given in Ref. [6] plots of the solution regions on the m_h - m_A plane for the old a_μ data with specific values of $\tan\beta$ and the scalar mixing angle α . We will present similar results here with, however, the complementary R_b constraint included. We will see that not much area of the parameter space can survive the combination of both a_μ and R_b data.

The current R_b measurement is given by [22]

$$R_b^{\text{exp}} = 0.21646 \pm 0.00065 .$$

With $R_b^{\text{SM}} = 0.215768$, we have

$$\Delta R_b \equiv R_b^{\text{exp}} - R_b^{\text{SM}} = 0.000692 \pm 0.00065 . \quad (19)$$

The ΔR_b contributions in the 2HDM are given, for example, by formulas in Ref.[23]. The charged Higgs contribution is always negative. On the other hand, there is a window of parameter space for the neutral Higgs contributions to be positive. From our discussions above, we need a light pseudoscalar and have to live with a heavy charged Higgs. We are therefore more interested in the neutral Higgs contributions.

Let us first focus on the contributions from the lighter Higgs bosons, the pseudoscalar A and the real scalar h , pushing the other scalar H to the heavy-mass limit together with H^\pm . The scenario will actually be well justified by our discussion on the constraint of the ρ parameter in the next section. The smallness of ΔR_b contributions admitted here generally disfavors a large mass splitting between m_h and m_A . This is in contrast to the requirement of a positive contribution to a_μ . Since the SM result (with $M_{H_{SM}}$ at 115 GeV) now represents a 3σ deviation in a_μ , better fits to the combined a_μ - R_b data are possible from the 2HDM. We illustrate some such fits in Fig. 3. In the figure, we take the case of $\tan\beta = 58$ and check various values of the Higgs mixing angle α . Here, and in the discussion below unless specifically stated otherwise, we stick to $m_{H^\pm} = 500$ GeV and $m_H = 1$ TeV. The exact value of m_H does not matter at all here, one, however, should note that the charged Higgs boson still gives a contribution of -2.32×10^{-4} to R_b , which is about $\frac{1}{3}\sigma$ in strength. Bearing this in mind, it is easy to estimate from our plots the slight shift in each of the admissible region as m_{H^\pm} is being pushed towards the decoupling limit.

² The plot is similar to the one given in Ref. [20], in which some more constraints are superimposed. We include here only the important ones. Note that the Tevatron exclusion region claimed in the paper is not used here. The exclusion result was from Ref.[21], which is an analysis based on the minimal supersymmetric standard model. The result should not be directly applicable to the present case of 2HDM. We do not find a similar study on the Tevatron data based on the 2HDM.

Each of the plots in Fig. 3 gives $\pm 2\sigma$ limits for a_μ and R_b fits, with darker shaded regions indicating the solution of interest defined by a total χ^2 of 4 or less. Also marked in the plots are regions with a total χ^2 less than the SM value of 10.3 (the sum of a_μ and R_b). The purpose of showing the area with a total $\chi^2 < \chi^2(\text{SM})$ is to indicate the region of parameter space that can fit the a_μ and R_b better than the SM, other than the decoupling limits. From now on, we concentrate on the dark area of a total $\chi^2 < 4$ as a valid solution to the a_μ and R_b data. We can see that there are no solutions for $-\frac{\pi}{8} < \alpha < \frac{\pi}{4}$. While a larger magnitude of the α looks more favorable, the best solution, with higher Higgs masses (m_h especially), stay close to $|\sin\alpha| = 1$, inclining more towards the negative sign. The most favorable range is around $-\frac{\pi}{2} < \alpha < -\frac{3\pi}{8}$ [*cf.* plots (c) and (d)]. The plots in Fig. 3 illustrate well the trend of the changes in the a_μ - R_b solution regions with variations in α , which is quite generic for $\tan\beta$ around and larger than 50. A higher m_h solution is preferred as the light mass solutions are easily killed by searches at LEP, including the DELPHI exclusion used in Fig. 2 and a particularly focused 2HDM analysis from OPAL[24], to be discussed below. In fact, as we will illustrate below, if any part of the solutions to the a_μ - R_b fits survive the exclusions from LEP, it is more or less the part with a high enough m_h value.³

For instance, the DELPHI exclusion we used in Fig. 2 obviously kills quite a part of the above solutions. At $\tan\beta = 58$, the lower bound on m_A is actually about 40 GeV. It is particularly interesting to check the case of a relatively small $\tan\beta$. We show in Fig. 4 the case of $\tan\beta = 40$, in which the DELPHI almost kills all solutions. In the figure, only a tiny window survives at $\sin\alpha = \frac{3\pi}{8}$. This is, however, at a m_h (as well as m_A) value too small to survive the OPAL exclusion discussed below. From the same study by DELPHI, the Yukawa processes were also used to impose bounds on the m_h [19]. Note that the plots in the Ref. [19] give bounds on Higgs masses versus the $b - \tau$ coupling enhancement factor, which is simply $\tan\beta$ for the pseudoscalar case, but has an added $|\sin\alpha|$ dependence for the case of the scalar h . In the range of m_A values of interest, however, the m_h bound is typically superseded by the OPAL exclusion. Note that the a_μ solution with m_h at a few GeV is also inadmissible, from the consideration of Υ -decay[6] and otherwise. Figure 4 also illustrates that a positive value of α , around $\frac{3\pi}{8}$ tends to give a_μ - R_b solutions with the largest m_A . This is mainly a result of the a_μ constraint. At a fixed m_h , the contribution of the scalar through the 2-loop Barr-Zee diagram to a_μ is suppressed by $|\sin\alpha|$, and thus allows a larger m_A . A slight asymmetry in the cases of positive and negative α values comes in as a result of the

³ In these plots, we used the standard R_b formulas for 2HDM as available in the reference [23] quoted. The formulas have not taken into consideration the possible tree-level decays of the Z^0 boson into a pair of Higgs states. Such very light Higgs regions are typically not of interest to theorists, as they would be easily excluded by direct searches. By the same token, we use the formulas as they are and show the a_μ - R_b fits without bothering about the tree-level modifications of R_b from such Higgs channels, leaving such fake solutions to be taken care of by the exclusions from LEP searches to be discussed below. We thank A. Sanda for alerting us to explicitly address the issue here.

different way the 1-loop contributions go.

We should also point out that we find no solutions to the a_μ - R_b fit at all for much lower $\tan\beta$. The a_μ solutions shown in Fig. 2 simply produce a m_h - m_A splitting too large to accommodate the R_b constraint. Therefore, the solutions to the a_μ - R_b fits start to emerge as $\tan\beta$ approaches a large enough value, not much below 40. To get solutions with high enough masses for the Higgs bosons so as to survive the exclusion limits from the LEP searches, one will have to get to a higher and higher $\tan\beta$ value. To check the details, we first turn to the powerful exclusions from OPAL.

Based also on the LEP data, OPAL has been publishing Higgs-search analyses specifically focused on the 2HDM. Here, we use the most recent results available [24, 25]. The results exclude a region at the lower left corner of the m_h - m_A plane for each specific value of the mixing angle α (four explicitly shown). As presented in Ref.[24], however, the results are not $\tan\beta$ specific. We show in Fig. 5 the solution regions from a_μ - R_b with the OPAL and the above mentioned DELPHI excluded regions superimposed. Here, we show the cases of $\tan\beta = 50$ and 58 for two α values, $-\frac{\pi}{4}$ and $\pm\frac{\pi}{2}$. The latter are chosen as they are among the α values for which the OPAL paper gives the explicit exclusion. The exclusion for non-specific α values only presents a substantially weakened result to be of interest here. The two α values are also close to or within the range of value for an optimal a_μ - R_b fit, as illustrated in Fig. 3 above.

In fact, the OPAL exclusions are based on the $\tan\beta$ value in the range 1 – 58, given only at four values of α , which we adopted here for the plots. An excluded point is one excluded at all value of $\tan\beta$ within the range. The excluded ranges may hence be extended at each specific value of $\tan\beta$, with more detailed analysis of the data[26]. In fact, one would expect the enhanced couplings at a larger $\tan\beta$ generally push the exclusion regions towards higher masses. One can see in the plots that the a_μ - R_b solution regions are largely cut off by the presented OPAL exclusions in general. Actually, nothing survives in the illustrated plots for $\tan\beta = 50$ [*cf.* plots (a) and (b) of Fig. 5]; and it is also quite obvious that the same is true for the case of $\tan\beta = 40$. Figures 4 and 5 together clearly illustrate the general trend of how the increase in $\tan\beta$ gives better results. While it does not do much for the case of $\alpha = -\frac{\pi}{4}$, at $\alpha = \pm\frac{\pi}{2}$, the admissible m_h and m_A values are pushed to be high enough to escape the OPAL exclusion at $\tan\beta > 50$ [*cf.* plot (c) of Fig. 5]. However, we are not bold enough to say for sure if no solution survives at $\tan\beta = 50$ though. The optimal case giving the largest m_h value for the a_μ - R_b is likely to be around $\alpha = -\frac{3\pi}{8}$, at which the present result of OPAL did not show its greatest strength.

We pick $\tan\beta = 58$ for the above detailed illustration of the a_μ - R_b fits because it gives the most favorable case within the limit of a direct application of the OPAL exclusion. There is apparently a surviving window in the parameter space. Combining our present study with a refined version of the OPAL analysis to focus on our a_μ - R_b solution regions, especially the upper blots as shown in plots (a) and (c) of Fig. 5, will certainly be very interesting. Exclusions have to be checked for each specific value of $\tan\beta$ and that of α . Such a study

will further narrow down the survival parameter space regions of the 2HDM, especially with further improved exclusion limits. We are told that the LEP data actually allows such an improvement[26]. A very tantalizing question is if the current constraints are actually strong enough to kill the model altogether!

The OPAL analysis is limited to $\tan\beta$ value at or below 58, while the DELPHI analysis stops at 100. The very large $\tan\beta$ region is theoretically unfavorable and may provide practical problems due to the much enhanced b -quark Yukawa coupling, which signals a breakdown of the perturbative treatment. Nevertheless, we will include some results from such uncomfortably large $\tan\beta$ values, and urge the OPAL group to push on a bit further in their analysis.

For $\tan\beta > 58$, we again illustrate some results for $\alpha = -\frac{\pi}{4}$ and $\pm\frac{\pi}{2}$ in Fig. 6, in which we still put in the (no longer exactly valid) OPAL exclusion from the $\tan\beta = 1 - 58$ scan for reference. For the $\alpha = -\frac{\pi}{4}$ case, the a_μ - R_b solution regions never rise above $m_h = 60$ GeV (as also for the smaller $\tan\beta$ cases), and partially excluded by DELPHI. There seem to be good enough reasons to believe that such low Higgs mass regions should be excluded by the available LEP data if an analysis along the OPAL line is performed. The $\alpha = \pm\frac{\pi}{2}$ case is better. The surviving region seen at $\tan\beta = 58$ moved further to the right, towards larger m_A , and further up a bit for larger m_h . The rise in m_h actually more or less saturates at $\tan\beta = 100$, and falls for even larger values of $\tan\beta$. Such a region still lives at the boundary of the DELPHI exclusion, but would still have a surviving part even if the OPAL exclusion can still be imposed. The region is, however, shrinking with increases in $\tan\beta$, due to a more fine-tuned a_μ - R_b solution. One should also bear in mind that the (upward) shifting, and hence slight enlargement, of this solution region with a further increase in the m_{H^\pm} value. For this purpose, we give the charged-Higgs contribution to R_b in Fig. 7.

Let us summarize our results so far. We have seen that combining the suggested requirement of producing a definite positive contribution to a_μ while keeping a limited deviation from the SM R_b result is an extremely stringent constraint on the parameter space of the 2HDM. When the available direct experimental search results from the LEP experiments are further implemented, there is at most a tiny window of parameter space that can survive. The apparently surviving region from the above discussions is restricted to very large values of $\tan\beta$. In fact, it may be already uncomfortably large, inviting the problem of the perturbativity of the Yukawa coupling of the b quark. As for the mixing angle α , it is being pushed close to the $-\frac{\pi}{2} < \alpha < -\frac{3\pi}{8}$ region. All these are based on a strong mass splitting between the charged Higgs and the light scalars, with the pseudoscalar A lying typically below 80 GeV and the scalar h below 140 GeV.

Recall that we have essentially decoupled the heavy Higgs boson H in the above analysis. We promised to justify this as a physics requirement. We first noted that a not too heavy H would more or less add to the effect of the other real scalar h in the contributions to a_μ and R_b . So, we expect it to ask for a larger mass splitting when fitting a_μ is concerned, but a smaller mass splitting to fit R_b . In another word, further tightening of the apparent solution

window. In the section below, we will show that fitting another precision EW parameter, the ρ parameter, actually does require sending m_H to a very large value, indeed well beyond m_H^\pm .

V. THE ρ PARAMETER CONSTRAINT

The parameter ρ was introduced to measure the relation between the masses of W^\pm and Z^0 bosons. In the SM $\rho \equiv M_W^2/M_Z^2 \cos^2\theta_W = 1$ at tree-level. However, the ρ parameter receives contributions from the SM corrections and from new physics. The deviation from the SM prediction is usually described by the parameter ρ_0 defined by[27]

$$\rho_0 \equiv \frac{M_W^2}{\rho M_Z^2 \cos^2\theta_W} , \quad (20)$$

where the ρ in the denominator absorbs all the SM corrections, including the corrections from the top quark and the SM Higgs boson. By definition, $\rho_0 = 1$ in the SM. Sources of new physics that contribute to ρ_0 can be written as

$$\rho_0 = 1 + \Delta\rho_0^{\text{new}} , \quad (21)$$

where $\Delta\rho_0^{\text{new}} = \Delta\rho^{\text{2HDM}} - \Delta\rho^{\text{SM-Higgs}}$ in our case. Note that since the two-doublet Higgs sector (in the 2HDM) is employed here to replace the SM Higgs, the latter contribution to $\Delta\rho$ has to be subtracted out.

The most recent reported value of ρ_0 is [13]

$$\rho_0 = 1.0004 \pm 0.0006, \quad (\text{with } M_{H_{\text{SM}}} \text{ fixed at } 115 \text{ GeV}) . \quad (22)$$

In terms of new physics the constraint becomes:

$$\Delta\rho_0^{\text{new}} = 0.0004 \pm 0.0006 . \quad (23)$$

In 2HDM $\Delta\rho$ receives contributions from all Higgs bosons given by [1, 28]

$$\begin{aligned} \Delta\rho^{\text{2HDM}} = & \frac{\alpha_{\text{em}}}{4\pi \sin^2\theta_W M_W^2} \left[F(m_A, m_{H^+}) + \cos^2(\beta - \alpha) [F(m_{H^+}, m_h) - F(m_A, m_h)] \right. \\ & \left. + \sin^2(\beta - \alpha) [F(m_{H^+}, m_H) - F(m_A, m_H)] \right] \\ & + \cos^2(\beta - \alpha) \Delta\rho^{\text{SM}}(m_H) + \sin^2(\beta - \alpha) \Delta\rho^{\text{SM}}(m_h) , \end{aligned} \quad (24)$$

where

$$\begin{aligned} F(x, y) &= \frac{1}{8}x^2 + \frac{1}{8}y^2 - \frac{1}{4} \frac{x^2 y^2}{x^2 - y^2} \log\left(\frac{x^2}{y^2}\right) = F(y, x) , \\ \Delta\rho^{\text{SM}}(M) &= -\frac{\alpha_{\text{em}}}{4\pi \sin^2\theta_W M_W^2} \left[3F(M, M_W) - 3F(M, M_Z) + \frac{1}{2}(M_Z^2 - M_W^2) \right] . \end{aligned} \quad (25)$$

Let us take a closer look into the implication of the formulas above. First of all, we note that $\Delta\rho^{\text{SM}}(M)$ has a negative value with magnitude increasing with M . As to be expected from above, the value is about -0.0004 at $M = 115$ GeV. It has a relatively mild variation, and does not go beyond -0.005 even as M gets to 10 TeV. In direct contrast, the other contributions to $\Delta\rho^{\text{2HDM}}$ in the above formula are very sensitive to the masses involved. The $F(x, y)$ function is always positive, vanishes only at $x = y$, and increases with a faster and faster rate with the splitting between x and y . In a typical scenario that is of interest here, we expect the pseudoscalar to be the lightest Higgs state with a quite heavy charged Higgs. That makes the contribution from the first term [involving $F(m_A, m_{H^+})$] large; indeed of order 0.01 for m_{H^+} satisfying the lower bound from $b \rightarrow s \gamma$ and $B - \bar{B}$ mixing. To get the required almost zero value of $\Delta\rho^{\text{2HDM}}$, we need some negative contributions from the terms involving $[F(m_{H^+}, m_h) - F(m_A, m_h)]$ and $[F(m_{H^+}, m_H) - F(m_A, m_H)]$. And the solution is obviously a fine-tuned one. Consider a case of degenerated Higgs real scalars, $m_H = m_h = M$. The $(\beta - \alpha)$ dependence in the formula is removed as the sine-square and cosine-square parts are combined. We need $[F(m_{H^+}, M) - F(m_A, M)]$ to have a negative value close in magnitude to that of $F(m_A, m_{H^+})$. The former is obviously positive roughly when M is closer to m_A than m_{H^+} , and negative when it is the other way round; and it can be larger than $F(m_A, m_{H^+})$ only for $M > m_{H^+}$. The $(\beta - \alpha)$ dependence comes back in the generic situation, with a mass splitting between the two real scalars. Obviously, at least one of them, by definition H , has to be heavy. However, they cannot be both heavy, because the R_b constraint does not allow only a light pseudoscalar giving a substantial contribution. Hence, this additional requirement of a limited splitting between m_A and m_h clearly suggests a large m_H , typically larger than m_{H^+} . The larger the m_H value, the smaller the $\sin^2(\beta - \alpha)$ is required. Admissible solutions, though fine-tuned, can be obtained so long as the required $\sin^2(\beta - \alpha)$ falls into the legitimate interval. A large splitting between m_H and m_h also resulted in a very narrow range of admissible $(\beta - \alpha)$ values, and hence the α values at a fixed $\tan\beta$ of interest.

Our numerical results corroborate well with the above analytical discussions. The latter is in some disagreement with discussions in Ref.[28] though. We illustrative our discussion with a plot in Fig. 8. Here, we take a ‘‘surviving’’ solution point to the a_μ - R_b fits and perform a further fitting together with the ρ parameter by varying m_H and m_{H^+} . The extremely fine-tuned nature of the solution is well-illustrated by the very narrow χ^2 bands. Moreover, m_H is always more than twice of m_{H^+} for an $|\sin\alpha|$ larger than 0.8. Note that $\sin\alpha$ of -0.8 and -0.92 roughly correspond to an α value of $\frac{-3\pi}{10}$ and $\frac{-3\pi}{8}$, respectively. The basic features remain if other solution points are taken, hence, we refrain from showing more plots.

VI. CONCLUSIONS

The requirement for the 2HDM II to give rise to the suggested $+3\sigma$ deviation in the muon anomalous magnetic moment demands a light pseudoscalar, preferably around 40 GeV for

$\tan\beta \leq 58$. The FCNC constraints, in particular the $b \rightarrow s\gamma$, require a heavy charged Higgs beyond 400 GeV. This large mass splitting in the Higgs mass spectrum is difficult to be accommodated by the precision EW measurements. In particular, the ρ parameter constraint then admits only very fine-tuned solutions, with cancellation from opposite contributions good to one in a hundred, favoring heavy real scalars. The fine-tuned nature of the solutions, while making many physicists uncomfortable with the model, is not in itself a good enough reason to pronounce the death of the model. If one has reasons to be confident about the correctness of the model, one would say that the available constraints are just strong enough to pin down for us the values of the unknown model parameter. A good example of such a situation is given by the pinning down of the top mass value from precision EW data prior to the experimental discovery of the top quark.

Nevertheless, we have not had much of a reason to believe in the correctness of the 2HDM. In fact, in our analysis here, we focus more on the simultaneous fits to Δa_μ and R_b . Having only the pseudoscalar contribution dominated the corrections to R_b is fatal. Hence, we require a relatively light m_h , while pushing m_H to way beyond m_{H^+} in order to satisfy the ρ parameter. Even then, not much of a solution to the a_μ - R_b fits survives the direct search exclusion. Here, we require a total χ^2 of 4 or smaller for the a_μ - R_b fits to claim a good solution. For roughly $\tan\beta < 40$, no solution to a_μ - R_b fits survives the DELPHI exclusion. In fact, there is no solution to the a_μ - R_b fit for a $\tan\beta$ value quite a bit smaller than 40. For $\tan\beta$ value from around 40 to a bit beyond 50, solutions surviving the DELPHI exclusions exist, but only to be killed by the OPAL exclusions. For even larger $\tan\beta$, the a_μ - R_b solutions surviving both the DELPHI and OPAL exclusions started to emerge. This is very much restricted to an α value in the range $-\frac{\pi}{2} < \alpha < -\frac{3\pi}{8}$. Solution regions shrink fast outside the range as the m_h values given by the a_μ - R_b fits drop towards OPAL exclusion bound.

In summary, under the strong restriction of the available constraints, we show that only a very tiny window of apparent solutions exist close to the limit of $\tan\beta \leq 58$. If the OPAL group could tailor their analysis of the LEP data to focus on the apparent solution window as shown here, we would be able to have a more definite conclusion. It looks to us that the solution window will be shut down quite substantially. So, we have “almost enough” constraints to kill the model altogether. For $\tan\beta$ beyond the 58 limit, our hands are tied at the moment by the unavailability of the strong LEP exclusion results as presented by OPAL. The very large $\tan\beta$ values certainly make many of us uncomfortable though. It is theoretical undesirable as limited by the blowing up of the bottom Yukawa couplings.

Acknowledgments

We thank D. Chang, C. Kao, W.-Y. Keung, and A. I. Sanda for valuable discussions. We are also in debt to P. Ferrari from OPAL and M. Boonekamp from DELPHI for clarification

about their results. This research was supported in part by the National Science Council grant number NSC91-2112-M-008-042 (O.K.) and by the NCTS.

Otto Kong thanks the hospitality of National Center for Theoretical Sciences, Taiwan during the early phase of the study, and that of KEK Theory Group, Japan where the final draft is finished.

-
- [1] *The Higgs Hunter's Guide* by J. Gunion *et al.*, Addison-Wesley, New York, 1990.
 - [2] S. Glashow and S. Weinberg, Phys. Rev. **D15**, 1958 (1977).
 - [3] M. Ciuchini, G. Degrassi, P. Gambino, and G.F. Giudice, Nucl. Phys. **B527**, 21 (1998).
 - [4] K. Chetyrkin, M. Misiak, and M. Münz, Phys. Lett. **B400**, 206 (1997); Erratum-*ibid.* **B425**, 414 (1998); A. Kagan, M. Neubert, e-Print Archive: hep-ph/9805303.
 - [5] D. Chang, W. Chang, C. Chou, and W. Keung, Phys. Rev. **D63**, 091301 (2001).
 - [6] K. Cheung, C. Chou, and O.C.W. Kong, Phys. Rev. **D64**, 111301 (2001).
 - [7] G. Buchalla, A. Buras, and M. Lautenbacher, Rev. Mod. Phys. **68**, 1125 (1996); A.J. Buras, M. Misiak, M. Münz, and S. Pokorski, Nucl. Phys. **424**, 374 (1994).
 - [8] B. Grinstein, R. Springer, and M. Wise, Nucl. Phys. **B339**, 269 (1990).
 - [9] T. Inami and C.S. Lim, Prog. Theor. Phys. **65**, 297 (1981); Erratum, *ibid.*, 1772.
 - [10] Plenary talk by A. Stocchi in ICHEP2002, July 2002, Amsterdam, Netherland.
 - [11] Plenary talk by M. Neubert in SUSY02, June 2002, DESY, Hamburg, Germany.
 - [12] L.F. Abbott, P. Sikivie, and M. B. Wise, Phys. Rev. D **21**, 1393 (1980); G.G. Athanasiu, P.J. Franzini, and F.J. Gilman, S.L. Glashow and E.E. Jenkins, Phys. Lett. **196B**, 233 (1987); Phys. Rev. D **32**, 3010 (1985); C.Q. Geng and J.N. Ng, Phys. Rev. D **38**, 2857 (1988).
 - [13] Particle Data Group (K. Hagiwara *et al.*), Phys. Rev. **D66**, 010001 (2002).
 - [14] M. Davier, S. Eidelman, A. Hocker, and Z. Zhang, e-Print Archive: hep-ph/0208177; E. de Rafael, e-Print Archive: hep-ph/0208251; K. Hagiwara, A.D. Martin, D. Nomura, and T. Teubner e-Print Archive: hep-ph/0209187. The exact numbers in Eq. (15) are taken from the version 1 of Davier et al. In their subsequent versions, they changed it to 33.7 ± 11.2 , which, however, has negligible effects on the results presented in this work.
 - [15] S. Barr and A. Zee, Phys. Rev. Lett. **65**, 21 (1990); see also J. Bjorken and S. Weinberg, Phys. Rev. Lett. **38**, 622 (1977).
 - [16] The available literature on the class of contributions is mainly on the closely related electric dipole moment calculations. A partial list is given by D. Chang, W.-Y. Keung, and T.C. Yuan, Phys. Rev. D **43**, R14 (1991); R.G. Leigh, S. Paban, and R.-M. Xu, Nucl. Phys. B **352**, 45 (1991); C. Kao and R.-M. Xu, Phys. Lett. **B296**, 435 (1992); D. Chang, W.S. Hou, and W.-Y. Keung, Phys. Rev. D **48**, 217 (1993).
 - [17] There are complicated gauge dependence notion when some of the class of diagrams are calculated separately. The photon Barr-Zee diagrams with fermions running in the second

loop form a gauge invariant set on their own. We thank Wai-Yee Keung for comments on the issue.

- [18] See, for example, A. Czarnecki and W.J. Marciano, *Phys. Rev. D* **64**, 013014 (2001).
- [19] DELPHI Collaboration (prelim), DELPHI 2002-037-CONF-571.
- [20] M. Krawczyk, hep-ph/0208076.
- [21] CDF and D0 Collaborations (M. Roco for the collaboration), FERMILAB-CONF-00-203-E, in Proceedings of ICHEP 2000, Osaka, Japan, 27 Jul - 2 Aug 2000.
- [22] The LEP Collaborations Electroweak Working Group, LEPEWWG/2002-01.
- [23] A. Denner *et al.*, *Z. Phys.* **C51**, 695 (1991).
- [24] OPAL Collaboration (prelim), P. Ferrari *et.al.*, Physics Note PN475, 2001.
- [25] Further update or improved results may soon be available — P. Ferrari, private communications.
- [26] P. Ferrari, private communications.
- [27] J. Erler and P. Langacker, in *Review of Particle Physics*, *Phys. Rev.* **D66**, 010001 (2002).
- [28] P. Chankowski, M. Krawczyk, and J. Zochowski, *Eur. Phys. J.* **C11**, 661 (1999).

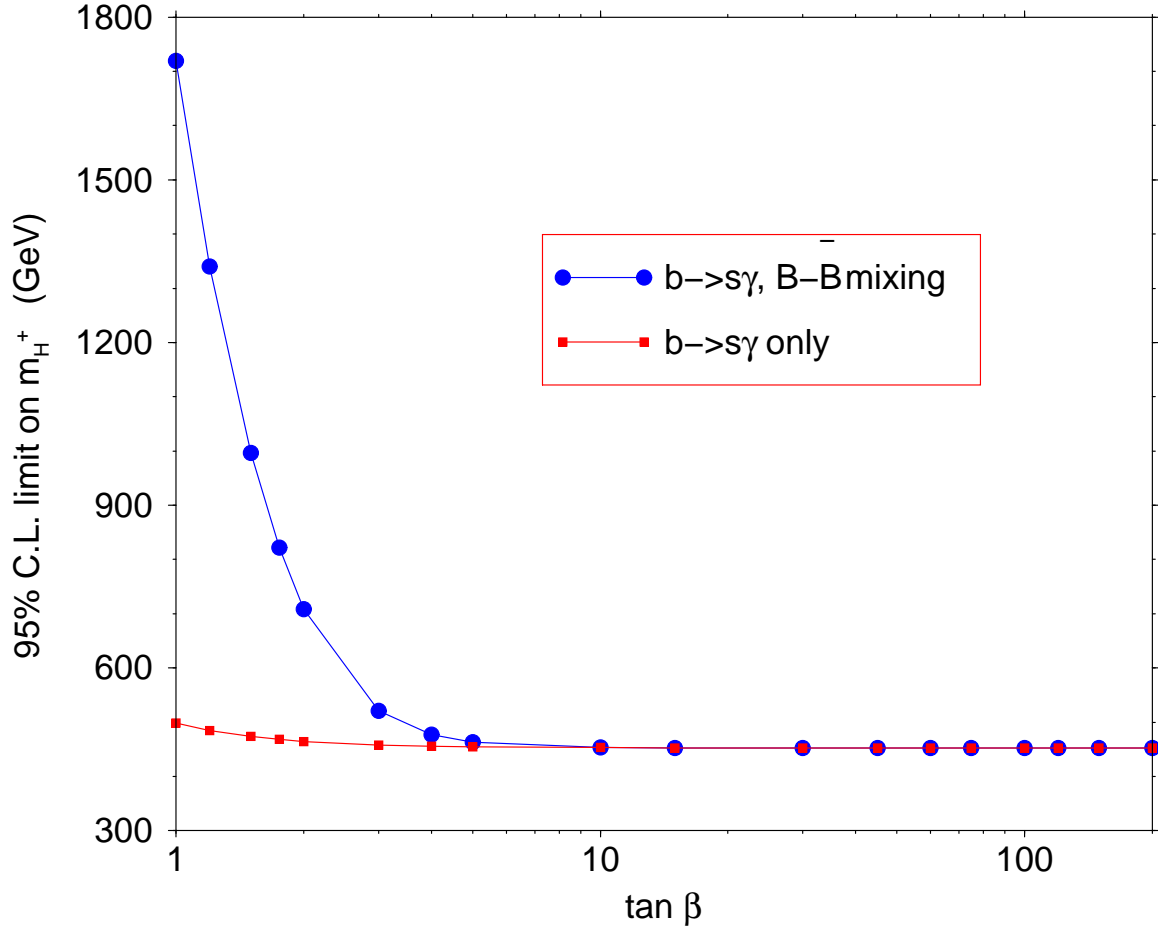


FIG. 1: 95% C.L. lower limit on the charged Higgs mass vs $\tan\beta$ due to the constraints on $b \rightarrow s\gamma$ and/or $B - \bar{B}$ mixing.

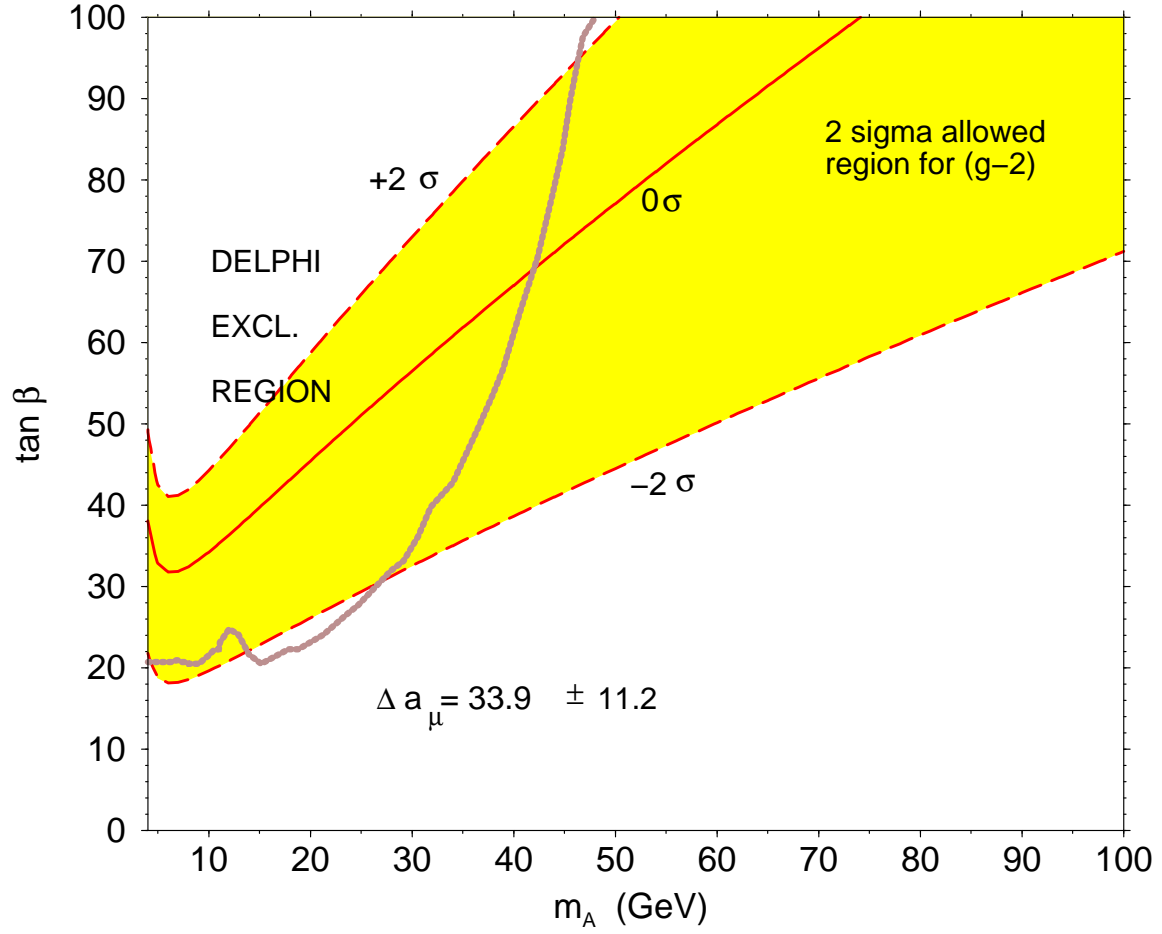


FIG. 2: The 2σ allowed region in the $(m_A, \tan\beta)$ plane due to the a_μ data. Here only the pseudoscalar contribution is considered. The DELPHI excluded region is represented by the thick line.

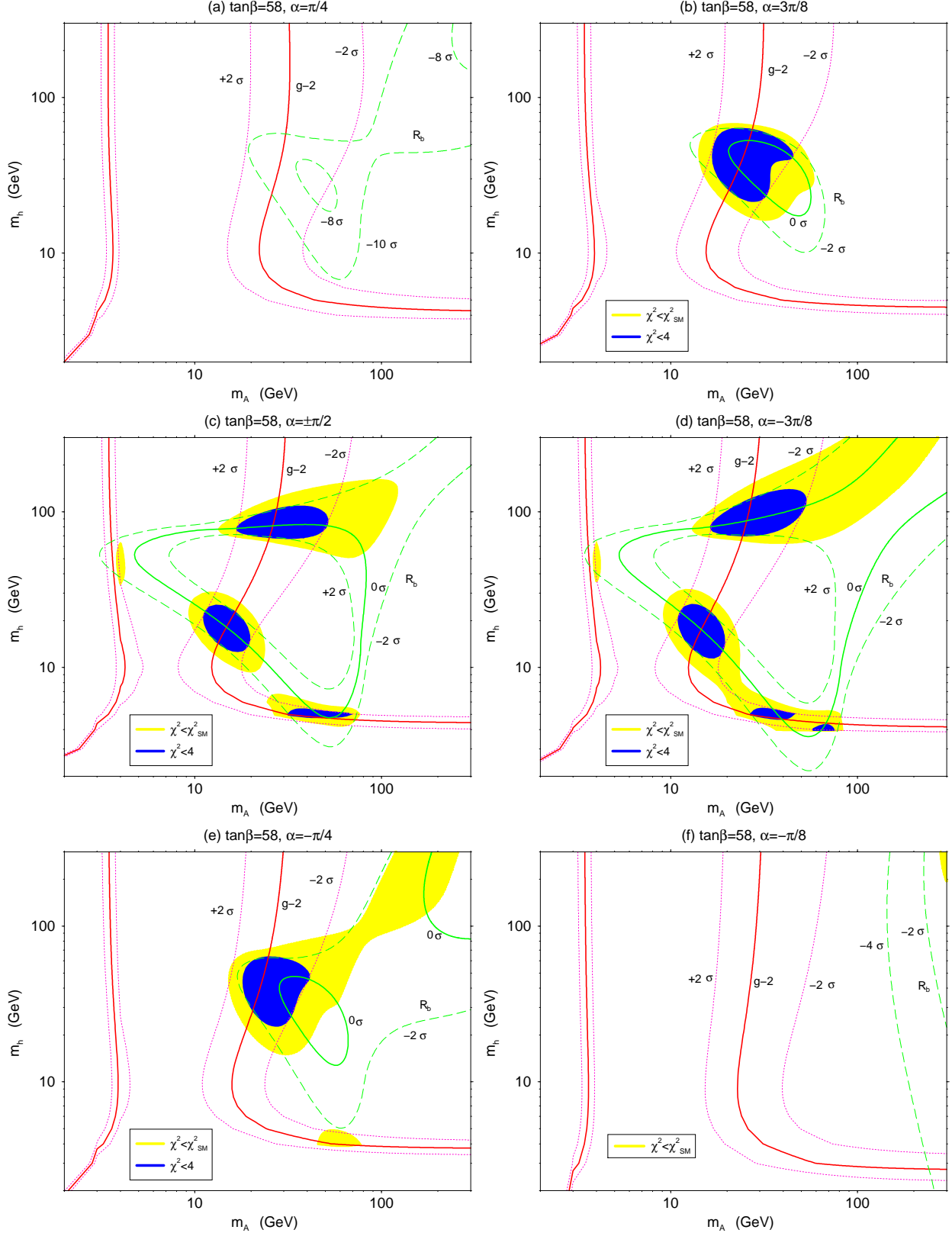


FIG. 3: The 2σ allowed regions in the (m_A, m_h) plane due to the constraints of a_μ and R_b for $\tan\beta = 58$. The smaller dark region is where the total χ^2 is less than 4 while the lighter region is where the total χ^2 is less than the $\chi^2(\text{SM}) = 10.3$.

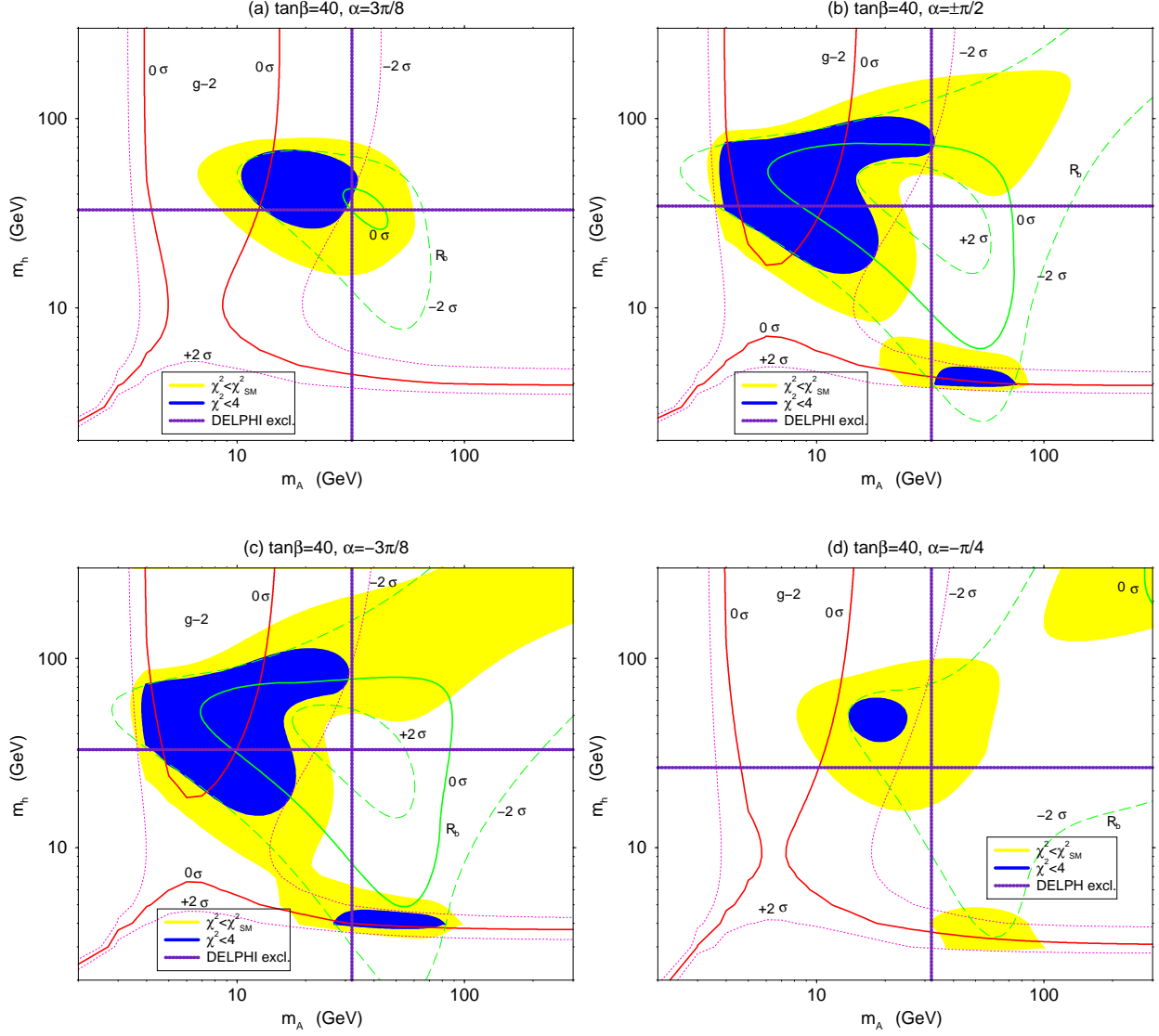


FIG. 4: The 2σ allowed regions in the (m_A, m_h) plane due to the constraints of a_μ and R_b for $\tan\beta = 40$. The smaller dark region is where the total χ^2 is less than 4 while the lighter region is where the total χ^2 is less than the $\chi^2(\text{SM}) = 10.3$. Here the lower mass limits on m_A and m_h from DELPHI are shown.

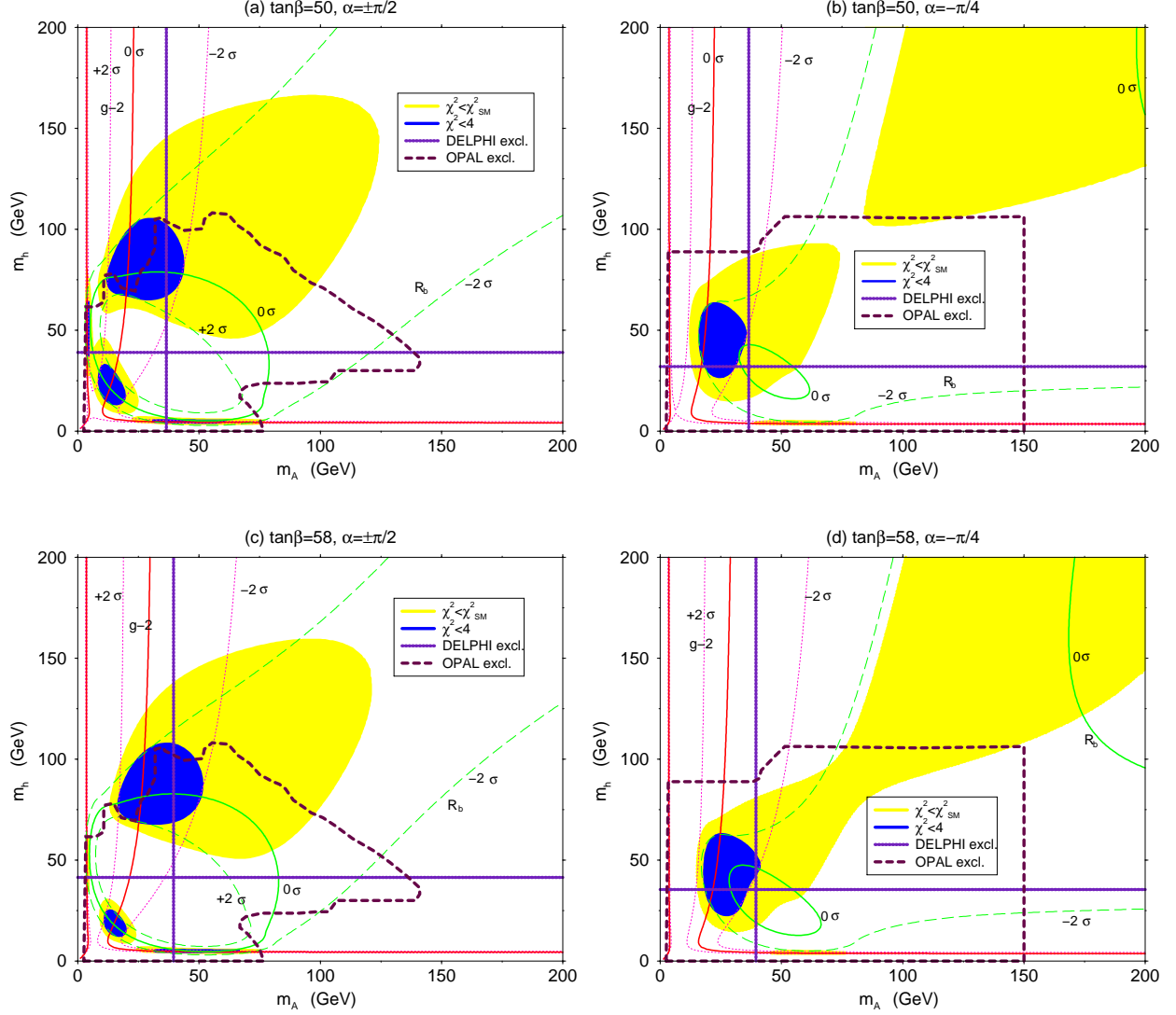


FIG. 5: The 2σ allowed regions in the (m_A, m_h) plane due to the constraints of a_μ and R_b for $\tan\beta = 50$ (a,b) and for $\tan\beta = 58$ (c,d). The smaller dark region is where the total χ^2 is less than 4 while the lighter region is where the total χ^2 is less than the $\chi^2(\text{SM}) = 10.3$. Here the lower mass limits on m_A and m_h from DELPHI, and the excluded region from OPAL are shown.

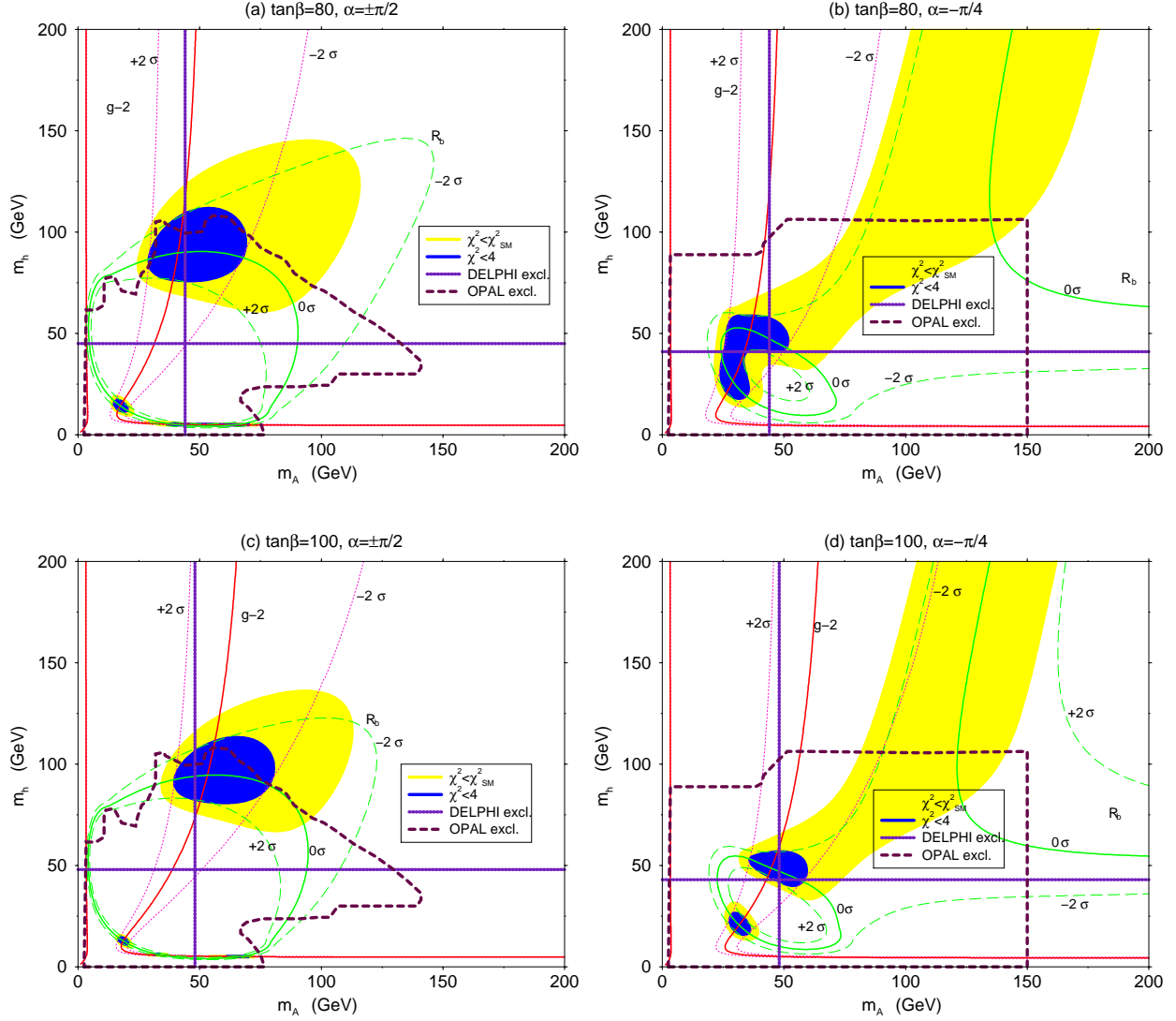


FIG. 6: Same as Fig. 5, but for $\tan\beta = 80$ (a,b) and for $\tan\beta = 100$ (c,d). Note that the OPAL exclusion regions put in is actually for $\tan\beta \leq 58$, hence no longer directly applicable here. In lack of the corresponding applicable results, they are kept here for reference.

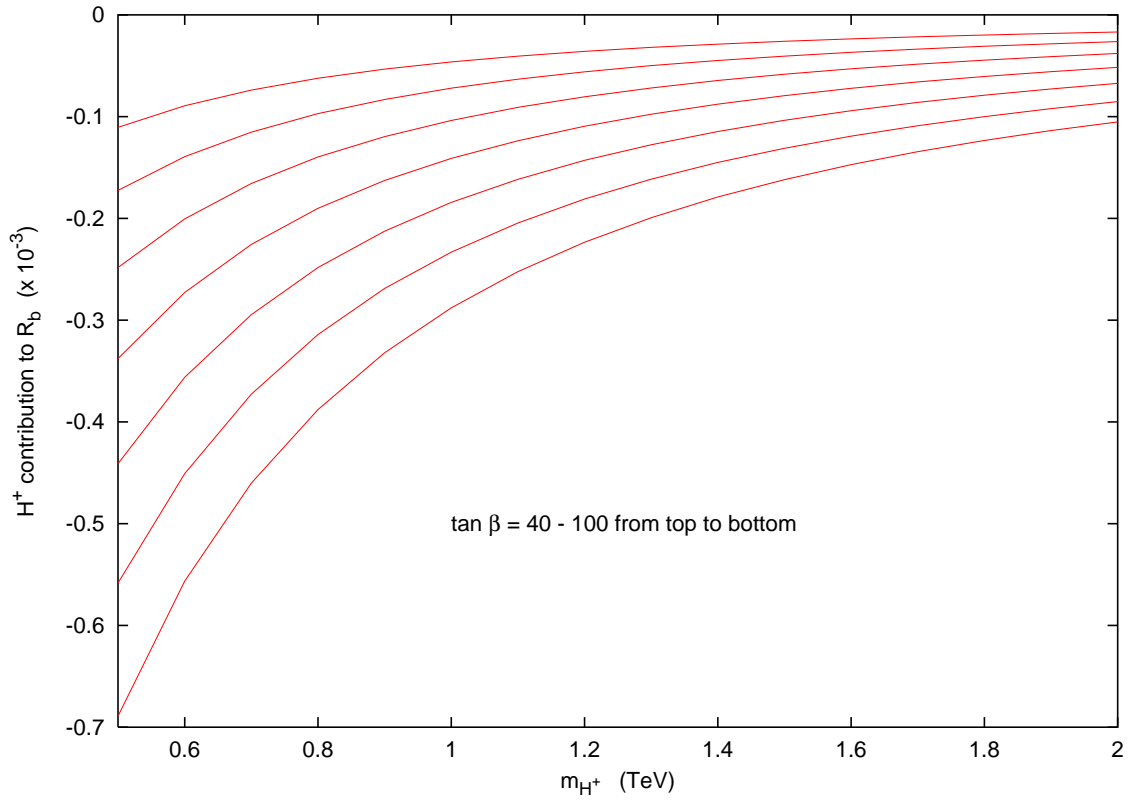


FIG. 7: The charged-Higgs contribution to R_b in units of 10^{-3} for $\tan\beta = 40 - 100$ (from the top to the bottom).

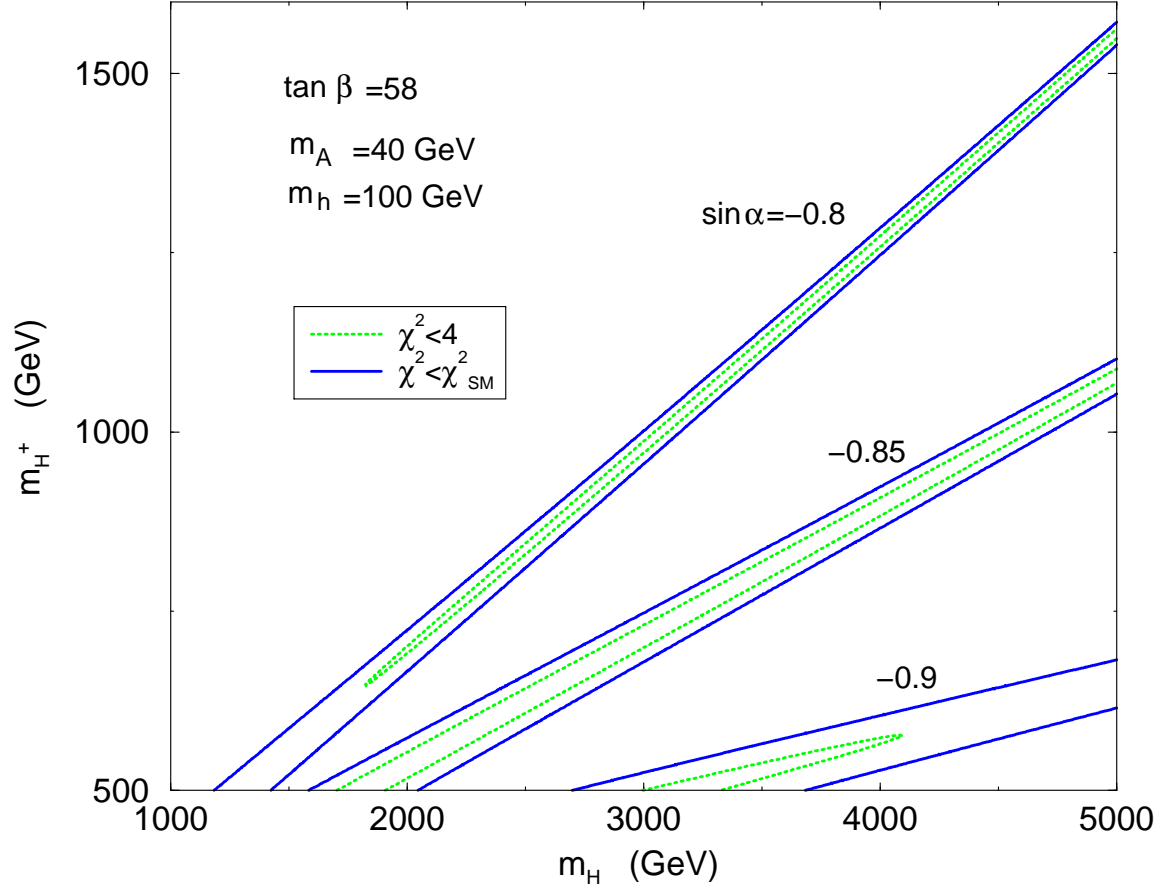


FIG. 8: The allowed region in the plane of (m_H, m_{H^+}) due to constraints of a_μ , R_b , and the ρ parameter. Here the $m_A = 40 \text{ GeV}$ and $m_h = 100 \text{ GeV}$ for $\tan \beta = 58$ are chosen from the allowed darker region in Fig. 5(c).